# The N-Terminal 1000 Residues of Apolipoprotein B Associate with Microsomal Triglyceride Transfer Protein to Create a Lipid Transfer Pocket Required for Lipoprotein Assembly†

Nassrin Dashti,[‡,§] Medha Gandhi,[||,§] Xiaofen Liu,[||,§] Xinli Lin,[⊥] and Jere P. Segrest*[,||,§,¶]

*Department of Medicine, Atherosclerosis Research Unit, Department of Nutrition Sciences, and the Department of Biochemistry and Molecular Genetics, University of Alabama at Birmingham Medical Center, Birmingham, Alabama 35294 and Oklahoma Medical Research Foundation, Oklahoma City, Oklahoma 73104*

*Received September 4, 2001; Revised Manuscript Received April 4, 2002*

ABSTRACT: Apolipoprotein (apo) B, the major protein component of the atherogenic low-density lipoprotein (LDL), has a pentapartite structure, $NH_2$-$\beta\alpha_1$-$\beta_1$-$\alpha_2$-$\beta_2$-$\alpha_3$-COOH, the $\beta$ domains containing multiple amphipathic $\beta$ strands and the α domains containing multiple amphipathic α helixes. We recently reported that the first 1000 residues of human apoB-100 have sequence and amphipathic motif homologies to the lipid-pocket of lamprey lipovitellin (LV) [Segrest, J. P., Jones, M. K., and Dashti, N. (1999) *J. Lipid Res. 40*, 1401−1416]. The lipid-pocket of LV is a small triangular space lined by three antiparallel amphipathic $\beta$ sheets, $\beta$A, $\beta$B, and $\beta$D. The $\beta$A and $\beta$B sheets are joined together by an antiparallel α helical bundle, α domain. We proposed [Segrest, J. P., Jones, M. K., and Dashti, N. (1999) *J. Lipid Res. 40*, 1401−1416] that formation of a LV-like lipid-pocket is necessary for lipid-transfer to apoB-containing lipoprotein particles and that this pocket is formed by association of the region of the $\beta\alpha_1$ domain homologous to the $\beta$A and $\beta$B sheets of LV with a $\beta$D-like amphipathic $\beta$ sheet from microsomal triglyceride transfer protein (MTP). To test this hypothesis, we generated four truncated cDNA constructs terminating at or near the juncture of the $\beta\alpha_1$ and $\beta_1$ domains: Residues 1−800 (apoB:800), 1−931 (apoB:931), 1−1000 (apoB:1000), and 1−1200 (apoB:1200). Characterization of particles secreted by stable transformants of the McA-RH7777 cell line demonstrated that (i) ApoB:800, missing the $\beta$B domain, was secreted as a lipid-poor aggregate. (ii) ApoB:931, containing most, but not all, of the $\beta$B domain, was secreted as lipid-poor particles unassociated with MTP. (iii) ApoB:1000, containing the entire $\beta$B domain, was secreted as a relatively lipid-rich particle associated hydrophobically with MTP. (iv) ApoB:1200, containing the $\beta\alpha_1$ domain plus 200 residues of the $\beta_1$ domain, was secreted predominantly as a lipid-poor particle but also as a minor relatively lipid-rich, MTP-associated particle. We thus have captured an intermediate in apoB-containing particle assembly, a lipid transfer competent pocket formed by association of the complete $\beta\alpha_1$ domain of apoB with MTP.

Apolipoprotein B (apoB)[1]-100, essentially the only protein component of the atherogenic low-density lipoprotein (LDL), has a pentapartite structure, $NH_2$-$\beta\alpha_1$-$\beta_1$-$\alpha_2$-$\beta_2$-$\alpha_3$-COOH, the $\beta$ domains containing multiple amphipathic $\beta$ strands and the α domains containing multiple amphipathic α helixes (*6*, *7*). The $\beta\alpha_1$ domain is a mixture of amphipathic $\beta$ strands and amphipathic α helixes (*7*) related to its structural homology to lamprey lipovitellin (LV) (*1*, *8*−*10*). The X-ray crystal structure of lamprey LV (*5*) is known to contain a lipid-pocket lined by three antiparallel amphipathic $\beta$ sheets designated $\beta$B, $\beta$A, and $\beta$D (*2*−*5*). The sheets $\beta$B and $\beta$A are joined together by a bundle of 17 α helixes, designated the α domain. A fourth $\beta$ sheet, $\beta$C, forms a globular $\beta$ barrel structure at the apex of the triangular lipid pocket (Figure 1).

Microsomal triglyceride transfer protein (MTP) is found in the lumen of the endoplasmic reticulum (ER) of predominantly hepatocytes and enterocytes (*11*). MTP is a heterodimer and consists of a 97-kDa large subunit that is essential for lipid transfer activity and a 58-kDa protein disulfide isomerase (PDI) that is required to keep the larger subunit in solution and to retain it in the ER (*12*, *13*). MTP is necessary for the formation of apoB-containing lipopro-

† This work was supported in part by the National Institutes of Health Grant R01 HL-63417.

* To whom correspondence should be addressed: Tel.: 205-934-4420; Fax: 205-975-8079; E- mail:segrest@uab.edu.

|| Department of Medicine, University of Alabama at Birmingham Medical Center.

§ Atherosclerosis Research Unit, University of Alabama at Birmingham Medical Center.

‡ Department of Nutrition Sciences, University of Alabama at Birmingham Medical Center.

¶ Department of Biochemistry and Molecular Genetics, University of Alabama at Birmingham Medical Center.

⊥ Oklahoma Medical Research Foundation.

[1] Abbreviations: apo, apolipoprotein; BSA, bovine serum albumin; DMEM, Dulbecco's modified Eagle's medium; EDTA, ethylenediaminetetraacetic acid; ER, endoplasmic reticulum; HDL, high-density lipoprotein; LDL, low-density lipoprotein; LV, lipovitellin; FBS, fetal bovine serum; MTP, microsomal triglyceride transfer protein; NDGGE, nondenaturing gradient gel electrophoresis; PAGE, polyacrylamide gel electrophoresis; PBS, phosphate-buffered saline; PDI, protein disulfide isomerase; SDS, sodium dodecyl sulfate; $S_d$, Stokes diameter.

10.1021/bi011757l CCC: $22.00 
Published on Web 05/09/2002

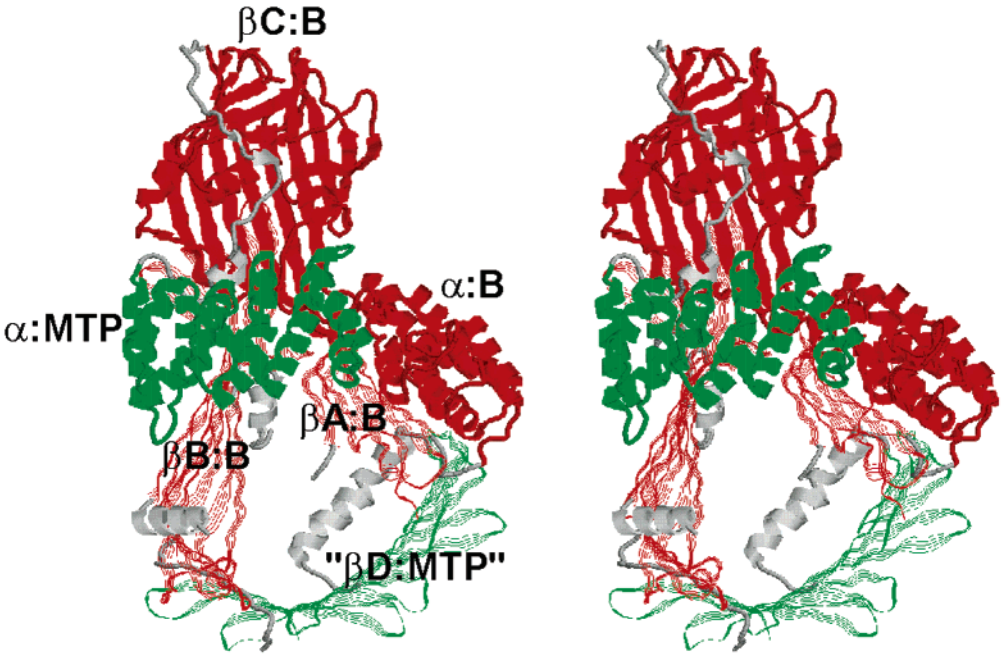


FIGURE 1: Homologue domains of human apoB and human MTP mapped onto a cross-eyed stereomodel of lamprey LV. The coordinates of the X-ray crystal structure for lamprey lipovitellin (*2*, *5*) were obtained from the Protein Databank (PDB). Domains of apoB locally homologous to LV ($\beta$C:B, α:B, $\beta$B:B, and $\beta$A:B) are indicated in red; domains of MTP locally homologous to LV (α:MTP and $\beta$D:MTP) are indicated in green. Individual $\beta$ strands of the $\beta$C domain ($\beta$ barrel) are represented by solid arrows with arrowheads denoting the C-terminal direction, α helixes, particularly the α helical domain, α, are represented by solid coils. The three $\beta$ sheet domains that create the lipid pocket, $\beta$B, $\beta$A, and $\beta$D, are represented by transparent $\beta$ strand ribbons. The figure was created using the program, RASMOL (*40*).

teins (*11*, *14*−*17*), through its direct association with the nascent apoB (*18*−*21*). This association has been shown to involve two electrostatic binding sites, one in the region of residue 200 of apoB (*10*, *22*) and a second in the region of residue 500 (*21*, *23*, *24*).

We recently proposed that formation of a LV-like lipid-pocket structural intermediate containing a nascent nucleus of lipid is required for initiation of assembly of apoB-containing lipoprotein particles (*1*, *7*, *25*). We suggested (*1*, *25*) that this pocket is formed via (i) electrostatic bonds of the $\beta\alpha_1$ domain of apoB with the $\beta$C and α domains of MTP (*10*, *21*−*24*) and (ii) hydrophobic association with the nascent lipid core of the region of $\beta\alpha_1$ homologous to the $\beta$A and $\beta$B sheets of LV and a surrogate $\beta$D amphipathic $\beta$ sheet derived from the C-terminal amphipathic $\beta$ strands of MTP (Figure 1).

To test the "lipid-pocket" model, we generated four progressively C-terminally truncated apoB cDNA constructs that terminated at or near the junction of the $\beta\alpha_1$ and $\beta_1$ domains. Characterization of the particles stably expressed and secreted in the rat hepatoma cell line McA-RH7777 allowed the capture of a stable intermediate in apoB-containing particle assembly, the lipid transfer competent pocket formed by the hydrophobic association of the first 1000 residues of apoB and MTP with a nascent nucleus of lipid.

## EXPERIMENTAL PROCEDURES

*Materials*. Cloning and restriction enzymes, fetal bovine serum (FBS), horse serum (HS), and antibiotic-antimycotic were obtained from GIBCO BRL Biological Company (Grand Island, NY). TOPO TA Cloning kit and precast Tris-Glycine gels were obtained from Invitrogen-Novex (Carlsbad, CA). Transfection MBS kit was from Stratagene (La Jolla, CA). Dulbecco's modified Eagle's medium (DMEM), trypsin, and G418 were purchased from Mediatech, Inc. (Herndon, VA). Fatty acid free bovine serum albumin (BSA) was from Miles Inc. (Kankakee, IL). Oleic acid (purity greater than 99% by capillary gas chromatography), sodium deoxycholate, Triton X-100, benzamidine, phenylmethylsulfonyl fluoride, leupeptin, aprotinin, and pepstatin A were from Sigma Chemical Co. (St. Louis, MO). Protein G-Sepharose CL-4B, L-[$^{35}$S]methionine, and Amplify were from Amersham Pharmacia Biotech. (Piscataway, NJ). Immobilin PVDF transfer membrane and Centriprep Centrifugal Filter devices YM-30 were purchased from Millipore Corp. (Bedford, MA). All reagents used for gel electrophoresis were from Bio-Rad Laboratories (Richmond, CA). Affinity purified polyclonal antibody to human apoB-100 was prepared in our laboratory and affinity purified polyclonal antibody to bovine MTP 97-kDa large subunit (*11*) was a generous gift from Dr. H. Jamil (Bristol-Myers Squib Pharmaceutical Research Institute, Princeton, NJ). The antibodies to apoB and MTP 97-kDa subunit were biotinylated at Brookwood Biomedical (Birmingham, AL). Monoclonal antibody to MTP 97-kDa large subunit and biotinylated goat anti-mouse immunoglobulin were obtained from BD Biosciences Pharmingen (San Diego, CA). ApoB-100 cDNA (*26*) was a gift from Gladstone Institute of Cardiovascular Disease, San Francisco, CA.

*Construction of Truncated apoB Expression Plasmids*. Truncated apoB cDNAs were prepared from pB100L-L (*26*) as a PCR template and the following primers (from 5′ to 3′): PCR-N:ATCGATATGGACCCGCCGAGGCCCGCGCTG; PCR-C1:ATCGATCTAAAGAAAAAAGTCATTCTTTGAGCC; PCR-C2:ATCGATCTACTCAATGAGAGGTGG-

GATGACCTC; PCR-C3: ATCGATCTATCTGTCCTCTCTCTG-GAGCTCATAGG; and PCR-C4: ATCGATCTAACCCACGT-GCCGGAAAGTCATGTCTG. PCR-N is the N-terminal primer and primers C1, C2, C3, and C4 are from the C-terminal position of the fragments; each pair of N- and C-terminal primers spans nucleotides 1−2481, 1−2874, 1−3081, and 1−3681, respectively, of the full-length apoB100 cDNA. The ClaI cloning sequence, which is not present in the apoB-100 cDNA fragment spanning nucleotides 1−3681, was installed at the 5′ end of all the primers to allow convenient cloning and a stop codon was installed in the C-terminal primers. The amplified PCR products were cloned into the TOPO TA cloning vector and used to transform cells. Clones harboring the vector were selected and identified by restriction enzyme digestion and nucleotide sequencing. The apoB fragments, 2481 bp (apoB:800), 2874 bp (apoB:931), 3081 bp (apoB:1000), and 3681 (apoB:1200) were excised from the vector, extracted, and purified, and ligated into the mammalian expression vector, the Molony murine leukemia virus based retrovirus LNCX (*27*) containing the neomycin phosphotransferase gene which confers G418 resistance for use as selectable marker. The apoB expression vectors, pLNCB:800, pLNCB:931, pLNCB:1000, and pLNCB:1200 were used to transform cells, and clones harboring plasmids containing apoB gene with the correct orientation were identified by restriction enzyme digestion and confirmed by nucleotide sequencing. These constructs were used to transfect mammalian cells.

*Cell Culture and Transfection*. The rat hepatoma McA-RH7777 cell line (American Type Culture Collection) was grown in DMEM containing 20% horse serum and 5% FBS as previously described (*28*). After 24 h, cells were transfected with 5 $\mu$g of DNA by calcium phosphate-mediated transfection using Stratagene Transfection MBS kit. Approximately 36 h post-transfection, cells were trypsinized, seeded onto 100-mm dishes and grown in DMEM containing serum and 0.8 mg/mL G418. Approximately 20−30 G418-resistant colonies from each transfection were chosen and tested for apoB expression by metabolic labeling and immunoblot analysis. One G418-resistant clone from each construct with the highest expression level of the corresponding apoB protein was selected, expanded in DMEM containing 20% horse serum, 5% FBS serum, and 0.2 mg/mL G418 and used for all subsequent studies.

*Metabolic Labeling Studies*. Clonal stable transformants of McA-RH7777 cells, expressing truncated forms of apoB, were grown as described above. At the start of experiments, the maintenance medium was removed, monolayers were washed twice with phosphate-buffered saline (PBS), and serum- and methionine-free DMEM containing either 0.75% BSA or 0.4 mM oleic acid bound to 0.75% BSA was added and the incorporation of [$^{35}$S]methionine into newly synthesized and secreted truncated forms of apoB during a 3 h incubation was determined by immunoprecipitation described below and in the figure legends.

*Immunoprecipitation*. After an overnight (17−20 h) incubation with serum-free medium or 3 h metabolic labeling with [$^{35}$S]methionine, the conditioned medium was collected, cells were washed with cold PBS and solubilized in nondenaturing lysis buffer as described (*19*, *28*). Preservative mixture at final concentrations of 500 units/mL penicillin-G, 50 $\mu$g/mL streptomycin sulfate, 20 $\mu$g/mL chloramphenicol, 50 $\mu$g/mL leupeptin, 50 $\mu$g/mL pepstatin A, 1.3 mg/mL $\epsilon$-amino caproic acid, 1 mg/mL EDTA, 1 mM benzamidine, 1 mM phenylmethylsulfonyl fluoride, and 100 kallikrein-inactivating units of aprotinin/mL was added to both medium and cell lysate to prevent oxidative and proteolytic damage (*19*, *28)*. The medium was centrifuged at 2,000 rpm for 30 min at 4 °C to remove broken cells and debris. The [$^{35}$S]-labeled apoB in the cell lysate and secreted into the medium or the unlabeled apoB-containing lipoprotein particles accumulated in the conditioned medium after an overnight incubation were immunoprecipitated under nondenaturing conditions (*19*, *22*, *28*) using polyclonal antibodies to either human apoB-100 or bovine MTP 97-kDa large subunit coupled to Protein G-Sepaharose CL-4B as previously described (*19*, *28*). The [$^{35}$S]-labeled apoB was extracted from Protein G by boiling for 4 min in sample buffer (0.125 M Tris-HCl, pH 6.8, 4% (w/v) SDS, 20% (v/v) glycerol, 10% (v/v) 2-mercaptoethanol, and 0.02% (w/v) bromophenol blue) and run on 4−12% sodium dodecyl sulfate polyacrylamide gel electrophoresis (SDS−PAGE) (*29*). After electrophoresis, the gels were analyzed by autoradiography or immunoblotting as described below and in the figure legends.

*Microsome Isolation*. After an overnight incubation with serum-free DMEM, conditioned medium was removed and processed as above. Cells were washed with cold PBS and disrupted by 20 passes through a Dounce homogenizer with a tight-fitting pestle in buffer containing 250 mM sucrose, 10 mM Tris-HCl, pH 7.4, 1 mM EDTA, and protease inhibitors described above. Intact cells and nuclei were removed by centrifugation at 10000*g*, for 10 min, and microsomes were isolated from the postnuclear supernatant as a pellet following centrifugation for 1 h at 100000*g*. The microsomes were treated with 0.1 M sodium bicarbonate, pH 11.5, on ice for 30 min to release the lumenal content. The truncated apoB-containing particles in the microsomal fraction and conditioned medium were detected by nondenaturing gradient gel electrophoresis (NDGGE) followed by immunoblotting as described below.

*Lipoprotein Isolation*. After an overnight incubation in serum-free DMEM, conditioned medium from seven 100-mm dishes was collected, preservative mixture was added, and medium was concentrated 10-fold using Centricon YM-30. The density of the medium was adjusted to 1.23 g/mL with solid KBr and lipoproteins ($d$ < 1.23 g/mL) were isolated by centrifugation for 40 h at 50 000 rpm. The lipoprotein fraction ($d$ < 1.23 g/mL) and infranatant ($d$ > 1.23 g/mL) were dialyzed against PBS and concentrated 2- and 10-fold, respectively, using Centricon YM-30 and analyzed by NDGGE and immunoblotting.

*Density Gradient Ultracentrifugation*. After an overnight incubation, conditioned medium from ten 100-mm dishes were collected, preservative mixture was added, and medium was concentrated 10-fold as above. The density of 10 mL of concentrated conditioned medium was adjusted to 1.36 g/mL with solid KBr, overlayered with 12 mL of $d$ = 1.26 g/mL and 18 mL of $d$ = 1.06 g/mL KBr solutions containing preservative mixture, and centrifuged for 6 h at 70 000 rpm at 7 °C (*30*). Forty fractions of 1.0 mL each were collected from the bottom of the centrifuge tube and after measuring their densities were analyzed by NDGGE and immunoblotting.

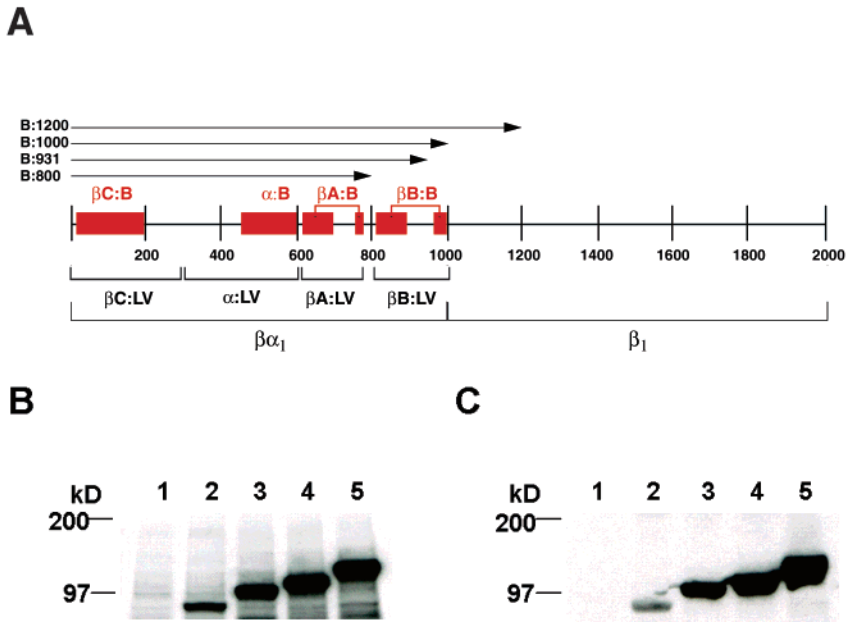


FIGURE 2: Location and stable expression of four truncated apoB constructs terminating at or near the junction of the $\beta\alpha_1$ and $\beta_1$ domains. Panel A is schematic diagram showing the location of the C-terminal truncation sites relative to the LV homologue domains. The domains of apoB homologous to LV, $\beta$C:B, $\alpha$:B, $\beta$A:B, and $\beta$B:B are shown as solid red boxes. The sequences of apoB outside the boxes (e.g., residues 300−450) may have structural similarity to LV but are not homologous. The location of the LV domains, $\beta$C:LV, $\alpha$:LV, $\beta$A:LV, and $\beta$B:LV are indicated below the sequence. The regions between the two separated $\beta$A:B and $\beta$B:B domains are not seen in the crystal structure and are presumably mobile. Expression plasmids encoding truncated forms of apoB were constructed as described in Experimental Procedures. ApoB:800, apoB:931, apoB:1000, and apoB:1200 denote amino acid residues 1−800, 1−931, 1−1000, and 1−1200, respectively, of the mature protein lacking the signal sequence. Panels B and C show stable expression of truncated forms of apoB in McA-RH7777 cells. Clonal cell lines of McA-RH7777 stably expressing the above truncated forms of apoB were generated as described in Experimental Procedures. After 4 days in culture, the maintenance medium was removed, cells were washed with PBS and incubated for 3 h in serum- and methionine-free DMEM containing 0.4 mM oleic acid bound to 0.75% BSA and [$^{35}$S]methionine (100 $\mu$Ci/mL of medium). The [$^{35}$S]-labeled apoB in cell lysate (panel B) and secreted into the medium (panel C) of LNCX (neo)-transfected (lane 1), apoB:800- (lane 2), apoB:931- (lane 3), apoB:1000- (lane 4), and apoB:1200- (lane 5) expressing cells was immunoprecipitated with anti-human apoB-100, applied to a 4−12% SDS−PAGE, and autoradiographed as described in Experimental Procedures.

*Nondenaturing Polyacrylamide Gradient Gel Electrophoresis (NDGGE)*. Total medium, lipoproteins ($d$ < 1.23 g/mL), infranatant ($d$ > 1.23 g/mL), and all 40 fractions from density gradient ultracentrifugation were run on 4−20% NDGGE for 48 h at 4 °C in buffer containing 24 mM Tris-HCl, pH 8.3 and 192 mM glycine and analyzed by immunoblotting.

*Immunoblot Analysis*. After SDS−PAGE or NDGGE, proteins were detected by Western blot analysis (*31*). Briefly, protein were transferred onto PVDF membrane using either Laemmli's transfer buffer system (*29*) for SDS−PAGE or buffer containing 25 mM Tris-HCl, pH 9.2, and 25 mM glycine for NDGGE. Membranes were blocked for 3 h in TBS buffer (100 mM Tris-HCl, pH 7.5 and 154 mM NaCl) containing 3% gelatin. After being washed with TTBS (TBS containing 0.1% Tween 20), membranes were incubated for 16 h with biotinylated antibodies to either human apoB-100 or bovine MTP 97-kDa subunit in TTBS containing 1% gelatin. Membranes were then washed with TTBS, incubated for 1 h with streptavidin-alkalin phosphatase conjugate, and developed using BioRad AP Conjugate Substrate kit.

## RESULTS

*Stable Expression and Secretion of C-Terminally Truncated Forms of ApoB*. Figure 2A is schematic diagram showing the location of the C-terminal truncation sites in reference to the LV "lipid pocket" homologue domains. The constructs are apoB:800 containing the $\beta$C, $\alpha$, and $\beta$A domains; apoB:931 containing the $\beta$C, $\alpha$, and $\beta$A domains, and most, but not all, of the $\beta$B domain; apoB:1000 containing the $\beta$C, $\alpha$, and $\beta$A domains, and all of the $\beta$B domain; and apoB:1200 containing the $\beta$C, $\alpha$, $\beta$A, and $\beta$B domains plus 200 residues of the $\beta_1$ domain. ApoB:800, apoB:931, apoB:1000, and apoB:1200 denote amino acid residues 1−800, 1−931, 1−1000, and 1−1200, respectively, of the mature protein lacking the signal sequence.

The expression and secretion of tuncated forms of apoB in stable transformants of McA-RH7777 cells are shown in Figure 2B,C. After a 3 h metabolic labeling with [$^{35}$S]-methionine, conditioned medium was harvested and preservative mixture was added; cells were solubilized in a nondenaturing lysis buffer containing preservatives. Aliquots of media and cell lysate were immunoprecipitated with anti-human apoB-100 under nondenaturing conditions and analyzed by SDS−PAGE and autoradiography. Results demonstrated the presence of [$^{35}$S]-labeled apoB in the cell lysate (Figure 2B) and the medium (Figure 2C) with the expected molecular weights of 92 kDa (apoB:800), 107 kDa (apoB:931), 115 kDa (apoB:1000), and 138 kDa (apoB:1200). On the basis of metabolic labeling and Western blot analysis (data not shown), the apoB:800 (N-terminal 17.6% of apoB-100) construct appeared to be expressed and secreted at a relatively lower rate compared to the other three constructs. We included apoB:800 in the present study to evaluate the role of the $\beta$B domain in the assembly of apoB-containing particles.

*MTP is Associated with the Cellular and Secreted Truncated Forms of ApoB.* The association of MTP with apoB has been previously reported (*10, 18*−*24*). We therefore sought to determine this association in our cell culture system. After a 17 h incubation in serum-free DMEM, conditioned medium was harvested, preservatives were added, and medium was concentrated 10-fold. Cells were washed and solubilized with nondenaturing lysis buffer containing preservatives. Aliquots of the concentrated medium and the cell lysate were immunoprecipitated with anti-MTP 97-kDa subunit under nondenaturing conditions. The immunoprecipitated proteins were run on SDS−PAGE and immunoblotted with anti-human apoB-100. Results of this two-step immunoprecipitation immunoblot analysis showed that antibodies to MTP 97-kDa subunit also precipitated truncated apoB proteins in both the cell lysate (Figure 3A) and medium (Figure 3B) indicating physical interaction between MTP and truncated forms of apoB.

To establish the interaction of MTP with newly synthesized and secreted apoB, cells were labeled with [$^{35}$S]-methionine for 3 h and conditioned medium was immunoprecipitated with anti-MTP 97-kDa subunit under nondenaturing conditions. The immunoprecipitated proteins were run on SDS−PAGE and subjected to autoradiography. Results demonstrated that all four truncated forms of apoB were immunoprecipitated with anti-MTP (Figure 3C). The faint band below the apoB band in Figure 3C might be MTP 97-kDa subunit but remains to be established. To confirm this apparent physical interaction between MTP and newly synthesized apoB, sequential immunoprecipitation experiments were carried out. Another aliquot of the above conditioned medium after metabolic labeling with [$^{35}$S]-methionine was immunoprecipitated with anti-MTP 97-kDa subunit under nondenaturing conditions. After the gels were washed extensively with nondenaturing buffer, the immunoprecipitated proteins were extracted by boiling the gels for 4 min with 0.05 mL of 2% SDS (*22*). The extracted proteins were diluted to 0.1% SDS with nondenaturing buffer, immunoprecipitated with anti-human apoB-100 as described above, and analyzed by SDS−PAGE and autoradiography. Results of this sequential immunoprecipitation shown in Figure 3D corroborated those obtained with the single-step immunoprecipitation (Figure 3C) and the two-step immunoprecipitation with anti-MTP followed by immunoblotting with anti-apoB-100 (Figure 3A,B) and established physical interaction between MTP and truncated forms of apoB both in the cells and medium. Results in Figure 3C show a band on top of the gel that was immunoprecipitated with anti-MTP 97-kDa subunit and corresponds to the molecular weight of apoB-48. The observation that this band was not detected after second immunoprecipitation with anti-human apoB-100 (Figure 3D), which does not cross-react with rat endogenous apoB (Figure 2B,C), is compatible with MTP being associated with rat endogenous apoB-48. Future studies are required to establish this possibility.

The identity of the putative MTP 97-kDa subunit secreted into the medium in association with truncated apoB proteins was further verified by immunoprecipitation with anti-human apoB-100 followed by immunoblotting with anti-MTP 97-kDa subunit. Aliquots of the concentrated medium were immunoprecipitated with anti-human apoB-100 under nondenaturing conditions. The immunoprecipitated proteins were run on SDS−PAGE and immunoblotted with polyclonal anti-MTP 97-kDa subunit. Results shown in Figure 3E demonstrated that antibody to human apoB-100 also precipitated MTP 97-kDa subunit in the conditioned medium of apoB:931-, apoB:1000-, and apoB:1200-expressing cells. In a parallel experiment, conditioned medium was immunoprecipitated with anti-human apoB-100 as described above and monoclonal anti-MTP 97-kDa subunit obtained from BD Biosciences Pharmingen (San Diego, CA) was used for

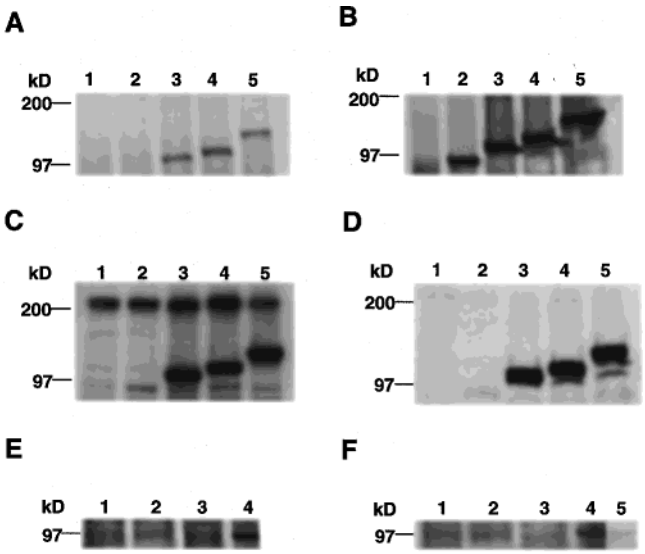


FIGURE 3: MTP is associated with C-terminally truncated forms of apoB in McA-RH7777 cells. In panels A and B, association of MTP with apoB in cells and medium was determined by immunoprecipitation with anti-MTP 97 kDa subunit followed by immunoblotting with anti-human apoB-100. McA-RH7777 cells stably expressing truncated forms of apoB were incubated with serum-free medium for 20 h. Conditioned medium was collected and concentrated and cells were solubilized in nondenaturing lysis buffer. Aliquots of cell lysate (panel A) and medium (panel B) from LNCX (neo)-transfected cells (lane 1), apoB:800- (lane 2), apoB:931- (lane 3), apoB:1000- (lane 4), and apoB:1200- (lane 5) expressing cells were immunoprecipitated with anti-MTP 97-kDa subunit under nondenaturing conditions as described in Experimental Procedures. The MTP-bound proteins were extracted and applied to 4−12% SDS−PAGE and were immublotted with anti-human apoB-100. In panel C, association of MTP with newly synthesized apoB was determined by a single-step immunoprecipitation. Cells were labeled with [$^{35}$S]methionine (100 $\mu$Ci/mL of medium) for 3 h and conditioned medium was immunoprecipitated with anti-MTP 97-kDa subunit under nondenaturing conditions. The MTP-bound [$^{35}$S]-labeled proteins were extracted from Protein G and applied to 4−12% SDS−PAGE and subjected to autoradiography. In panel D, interaction of MTP with apoB was determined by sequential immunoprecipitation. In the first step, conditioned medium from the above metabolic labeling with [$^{35}$S]methionine was immunoprecipitated with anti-MTP 97-kDa subunit under nondenaturing conditions. In the second step, the MTP-bound immunoprecipitated labeled proteins were extracted from Protein G as described in Experimental Procedures and were immunoprecitated with anti-human apoB-100 as described above. The [$^{35}$S]-labeled immunoprecipitated apoB was extracted from the Protein G, applied to 4−12% SDS−PAGE, and autoradiographed. In panels E and F, the association of MTP with apoB in medium was verified by immunoprecipitation of conditioned medium from apoB:931- (lane 1), apoB:1000- (lane 2), and apoB:1200- (lane 3) expressing cells with anti-human apoB-100 followed by immunoblotting with both polyclonal (panel E) and monoclonal (panel F) anti-MTP 97-kDa subunit as described for panels A and B. Lane 4 in panels E and F is MTP positive control provided by BD Biosciences and lane 5 in panel F is the extract of apoB:1000-containing band excised from a 4−20% NDGGE.

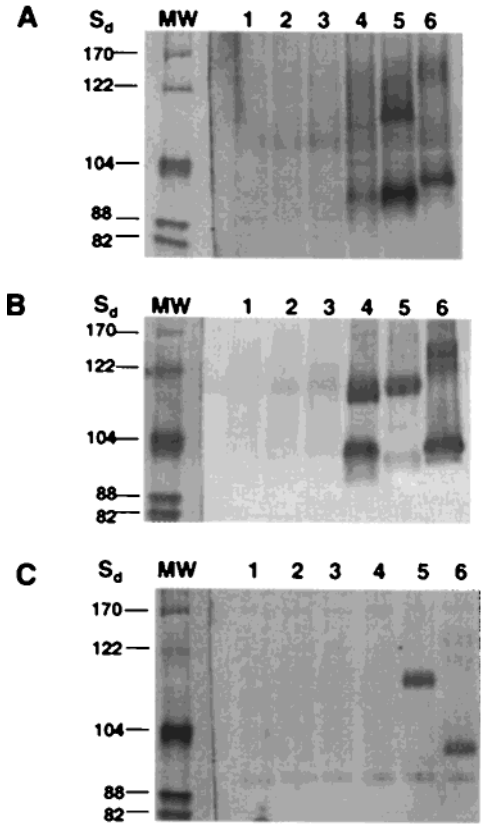


FIGURE 4: Truncated apoB-containing particles are formed in microsomes and are secreted into the medium. After incubation of cells with serum-free medium for 20 h, conditioned medium was collected and concentrated, and microsomes were isolated from the cells. In panel A, aliquots of microsomal fraction isolated from parental nontransfected McA-RH7777 cells (lane 1), LNCX (neo)-transfected cells (lane 2), apoB:800- (lane 3), apoB:931- (lane 4), apoB:1000- (lane 5), and apoB:1200- (lane 6) expressing cells were subjected to a 4−20% NDGGE at 4 °C for 48 h. Proteins were transferred onto PVDF membrane and detected by immunoblotting with anti-human apoB-100. In panel B, aliquots of the concentrated conditioned medium from each cell line was applied to a 4−20% NDGGE at 4 °C for 48 h and immunoblotted with anti-human apoB-100 as described above. In panel C, concentrated conditioned medium was applied to 4−20% NDGGE at 4 °C for 48 h and immunoblotted with anti-MTP 97-kDa subunit as described above.

immunoblotting. The results of this experiment (Figure 3F) corroborated the observation obtained with polyclonal anti-MTP 97-kDa subunit (Figure 3E). The above studies provide strong support for physical interaction between MTP and truncated forms of apoB secreted into the medium.

*Truncated ApoB-Containing Particles Are Formed in Microsomes and Are Secreted into the Medium*. We next examined the ability of the C-terminally truncated apoB species to form particles and determined their site of formation. To achieve this, cells were incubated overnight in serum-free medium, conditioned medium was harvested and, after addition of preservative mixture, was concentrated 10-fold. Cells were washed with PBS and microsomes were isolated as described in Experimental Prodedures. Aliquots of microsomal fraction were applied to 4−20% NDGGE and apoB-containing particles were visualized by immunoblotting. As shown in Figure 4A, we did not detect apoB-containing particles in the microsomes of parental nontransfected McA-RH7777 cells, LNCX (neo)-transfected cells, or apoB:800 (N-terminal 17.6% of apoB-100)-expressing cells. On the other hand, apoB:931 (N-terminal 20.5% of apoB-100), apoB:1000 (N-terminal 22% of apoB-100), and apoB:1200 (N-terminal 26.5% of apoB-100) truncated forms of apoB formed particles as detected with anti-human apoB-100 (Figure 4A). Analysis of the conditioned medium by NDGGE and immunoblotting with anti-human apoB-100 demonstrated that, as in the microsomes, no apoB-containing particles were detected in the conditioned medium of the nontransfected, neo-transfected, or apoB:800-expressing cells (Figure 4B). On the other hand, apoB:931-, apoB:1000-, and apoB:1200-expressing cell lines each secreted a single major and several minor apoB-containing particles (Figure 4B) with the same Stokes diameter ($S_d$) as those detected in the microsomes. The higher level of apoB:1000 small particle in the microsomes relative to that in the conditioned medium might be due to intracellular degradation in the absence of exogenous fatty acid and remains to be established.

Since our metabolic studies showed interaction between MTP and apoB in both the cells and medium, we examined potential association of MTP with the secreted intact truncated apoB-containing particles. Immunoblot analysis of the media with anti-MTP 97-kDa subunit demonstrated the presence of MTP only with apoB:1000- and apoB:1200-containing particles (Figure 4C). A doublet with a $S_d$ of approximately 92 Å was seen in all samples that presumably represents free MTP. Whatever its origin, the secretion of this doublet into the media is independent of whether the McA-RH7777 cells are expressing human apoB constructs.

*Ability of ApoB:931, ApoB:1000, and ApoB:1200 to Form Lipoproteins.* To determine the effect of different domains of the N-terminal 26.5% of apoB-100 on the density of the secreted apoB-containing particles, cells were incubated overnight in serum-free DMEM. Conditioned media and lipoproteins ($d$ < 1.23 g/mL) and infranatant ($d$ > 1.23 g/mL) isolated from there were analyzed by NDGGE and immunoblotting with antibodies to apoB-100 and MTP 97-kDa subunit. Because apoB:800 did not form particles (Figure 4B), it was not analyzed in this series of experiments. As shown in Figure 5, apoB:931-, apoB:1000-, and apoB:1200-expressing cell lines each secreted a single major apoB-containing particle with $S_d$ of 110, 112, and 99 Å, respectively. Several minor apoB-containing particles were also produced: ApoB:931 produced two minor particles with $S_d$ of 96 and 118 Å. ApoB:1000 produced a single minor particle with a $S_d$ of 95 Å, the major 112 Å particle appearing monodisperse. ApoB:1200 produced two minor particles with $S_d$ of 120 and 125 Å, thus creating a doublet.

Ultracentrifugation at $d$ = 1.23 g/mL showed further differences in the properties of the apoB-containing particles produced by the three cell lines. Only a minor fraction of the particles formed by apoB:931 floated (compare lane T with lane B in Figure 5A), indicating they are mostly lipid-poor. For the apoB:1000- and apoB:1200-expressing cell lines, there was significant flotation of the larger apoB-containing particles (112 and 120/125 Å, respectively), suggesting that they are relatively lipid-rich, while the smaller apoB-containing particles (95 and 99 Å, respectively), appear to be lipid-poor, although a minor fraction of the smaller apoB:1200 particle floated. The apoB:1000-expressing cell line was unique in that only the larger, apparently monodisperse, apoB-containing particle floated (Figure 5B). Consistent with results shown in Figure 4C, MTP was not

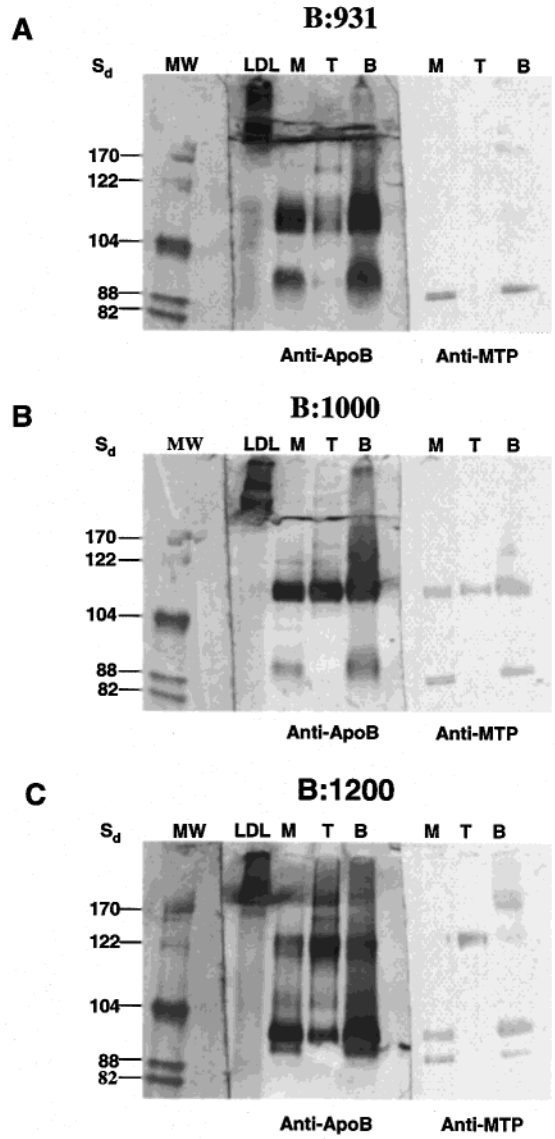


FIGURE 5: Analysis of the apoB:931-, apoB:1000-, and apoB:1200-containing particles secreted by stably transfected McA-RH7777 cells. After 4 days in culture, cells were washed with PBS and incubated for 20 h in serum-free DMEM containing 0.4 mM oleic acid bound to 0.75% BSA. The density of the concentrated conditioned medium from apoB:931- (panel A), apoB:1000- (panel B), and apoB:1200- (panel C) expressing cells was adjusted to 1.23 g/mL and lipoproteins were isolated by centrifugation for 40 h at 50 000 rpm. The lipoproteins ($d$ < 1.23 g/mL) and the entire infranatant ($d$ > 1.23 g/mL) were isolated and dialyzed against PBS containing preservatives and concentrated as described in Experimental Procedures. Aliquots of total medium (M), top $d$ < 1.23 g/mL fraction (T), and bottom $d$ > 1.23 g/mL fraction (B) were applied to a 4−20% NDGGE at 4 °C for 48 h. Proteins were transferred onto PVDF membrane and detected by immunoblotting with anti-human apoB-100 (left panel) and anti-MTP 97-kDa subunit (right panel).

detected in apoB:931-containing particles (Figure 5A). However, both of the larger apoB-containing particles secreted by the apoB:1000- and apoB:1200-expressing cell lines (112 and 125 Å, respectively) comigrated with anti-MTP bands (Figure 5B,C). The 99 Å particle, which is the major particle secreted by the apoB:1200-expressing cell line, also comigrated with an anti-MTP band (Figure 5C).

To confirm the association of MTP with apoB:1000-containing particles, conditioned medium was run on 4−20% NDGGE as described above. The band corresponding to apoB:1000 was excised from the gel and homogenized in PBS. The homogenate was adjusted to 1% SDS, and proteins were extracted by boiling the gel for 4 min. The extracted proteins were run on SDS−PAGE and immunoblotted with anti-human apoB-100 and monoclonal anti-MTP 97-kDa subunit. Both MTP 97-kDa subunit (Figure 3F, lane 5) and apoB:1000 (data not shown) were detected. The above results confirmed the presence of apoB-associated MTP in the medium.

*Amino Acids 931−1000 of ApoB-100 Are Critical for the Formation of a Lipidated Particle*. The density gradient distribution of the secreted apoB:931-, apoB:1000-, and apoB:1200- expressing cells is shown in Figure 6. All 40 fractions isolated by density gradient centrifugation were subjected to NDGGE and analyzed by immunoblotting with anti-human apoB-100. These results confirmed the results of the flotation experiments (Figure 5), and in addition, provided information about the mean density and size/density distribution of individual apoB-containing particles. Each of the truncated apoB species exibited a characteristic density distribution. The major apoB-containing particle formed by apoB:931 (Figure 6A) had a constant diameter of 110 Å across a wide range of densities and a mean density of 1.25 g/mL; thus, this particle is denser than the traditional high-density lipoprotein (HDL) density range of 1.063−1.21 g/mL. The small (96 Å) apoB:931-containing particles had a mean density of 1.28 g/mL. The large apoB-containing particle formed by apoB:1000 (Figure 6B) had a diameter that remained relatively constant at approximately 112 Å across a wide range of densities and a mean density of 1.208 g/mL that is within the $HDL_3$ density range of 1.125−1.21 g/mL; these particles also contained MTP (data not shown). Thus, over a short stretch of 69 residues from apoB:931 to apoB:1000, the nature of the secreted particle changed from a lipid-poor protein to a $HDL_3$-like lipoprotein. The small (95 Å) minor apoB:1000-containing particles had a mean density of 1.29 g/mL. Finally, the large apoB:1200 particle (Figure 6C) had a diameter that increased with decreasing density, ranging from 118 to 127 Å, and a mean density of 1.197 g/mL that is within the $HDL_3$ density range; however, the small apoB:1200 particle had a constant diameter of 99 Å and a non-HDL density of 1.24 g/mL (Figure 6C).

## DISCUSSION

One often quoted mechanism for the physical assembly of lipid particles containing apoB is the budding oil droplet (*32*). In this model, the N-terminal portion of apoB is embedded in the inner monolayer of the endoplasmic reticulum (ER) membrane, where it nucleates an oil droplet from the supersaturated rough ER membranes. Upon completion of apoB synthesis, this oil-droplet is detached from the bilayer to form the nascent lipoprotein. However, thermodynamic considerations make it unlikely that lipoproteins assemble through the wholesale remodeling or dismantling of membrane bilayers. The data presented here indicate that gradual lipid transfer into an apoB-containing particle during biosynthesis requires translocation of a critical length of apoB sequence necessary for creation of a competent lipid pocket.

The apoB:800-expressing cell line secretes an apoB fragment of the expected length. The fact that no apoB-

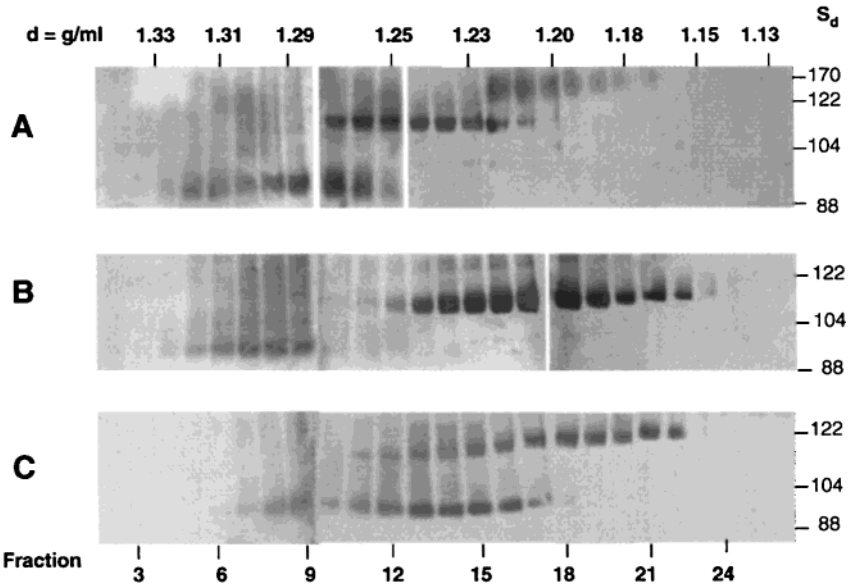


FIGURE 6: Density gradient ultracentrifugation distribution of (A) apoB:931-, (B) apoB:1000-, and (C) apoB:1200-containing particles secreted by McA-RH7777 cells. Cells were grown and incubated for 20 h under experimental conditions described in the legend to Figure 5. The density of 10 mL of concentrated conditioned medium was adjusted to 1.36 g/mL with solid KBr, overlayered with 12 mL of $d = 1.26$ g/mL and 18 mL of $d = 1.06$ g/mL KBr solutions containing preservative mixture, and centrifuged for 6 h at 70 000 rpm. Forty fractions of 1.0 mL each were collected from the bottom of the centrifuge tubes, and their densities were measured. Aliquots of fractions were applied to a 4−20% NDGGE and immunoblotted with anti-human apoB-100 as described in the legend to Figure 5. Fractions 27−40 did not show any apoB and are therefore not included in the figure.

containing particle is detectable in the media by Western blot analysis on NDGGE suggests that apoB:800 is likely secreted as an aggregate (or perhaps is associated with lipid droplets (*33*)) and thus fails to enter the gel. The apoB:931-expressing cell line secretes a 110 Å lipid-poor particle that contains little, if any MTP. The apoB:1000-expressing cell line secretes a monodisperse 112 Å particle containing both apoB:1000 and MTP plus sufficient lipid to have an $HDL_3$ density. The apoB:1200-expressing cell line secretes an $HDL_3$-like particle that, although larger and more buoyant than the apoB:1000-containing particle, is secreted in a lower concentration than a smaller lipid-poor apoB:1200-containing particle; both lipid-rich and lipid-poor apoB:1200 particles contain MTP.

The similarity of the apparent $S_d$ of the lipid-poor apoB:931 particle (110 Å) and that of the lipid-rich apoB:1000 particle (112 Å) requires an explanation. Since these $S_d$ were measured by NDGGE, particle shape influences the apparent $S_d$ more that particle mass; i.e., an elongated particle will have a greater apparent $S_d$ than a spheroidal particle of the same mass. Thus, we suggest that the 110 Å particle containing a collapsed, empty lipid pocket may be more asymmetric in shape than the 112 Å particle containing a loaded lipid pocket.

An interesting finding of this study was detection of MTP-bound apoB-containing lipoproteins in the medium. This is the first time, to the best of our knowledge, that the secretion of MTP-bound apoB-containing particles has been demonstrated. Since MTP is a microsomal protein (*11*), its secretion into the medium presents a biological paradox. However, several lines of evidence provide support for this novel observation: (i) Studies in HepG2 cells (*19*, *22*) have demonstrated physical interaction between MTP and apoB-100 in the cells, indicating that MTP remains with apoB throughout its maturation. (ii) Studies by Swift et al. (*34*) have demonstrated the presence of MTP within the Golgi content of mouse liver indicating that MTP is transported to the Golgi, potentially in association with apoB. (iii) Studies by Bradbury et al. (*23*) have shown a common binding site on MTP for apoB and PDI. (iv) Hussain et al. (*35*, *36*) have demonstrated that there is a strong interaction between MTP and human plasma LDL as well as truncated forms of apoB secreted by McA-RH7777 cells, that relative to MTP, there is a poor interaction between PDI and LDL (*35*), and that MTP binds to lipid vesicles and has a stronger affinity for LDL than lipid-free MTP (*36*).

The above studies are relevant to our results demonstrating the interaction between MTP and truncated forms of apoB in both the cells and medium, the existence of intact apoB:1000- and apoB:1200-containing particles in microsomes, and detection of MTP-bound apoB:1000- and apoB:1200-containing particles in the medium. It is therefore plausible that the apoB-containing particles found in the microsomes and transported into the Golgi (*34*) would be secreted into the medium. It can be speculated (*23*) that the binding of apoB to MTP displaces PDI, which retains MTP in the microsomes, thus allowing MTP to be secreted into the medium. Future experiments involving characterization of particles in subcellular compartments and localization of PDI are needed to establish this mechanism.

The observation that MTP is secreted into the medium associated with apoB raises two important issues that need to be addressed. First, our results tend to suggest that one molecule of MTP would bind to one molecule of apoB. Our attempt to confirm a 1:1 molar ratio of MTP to apoB in the medium using amino acid sequencing technique has not been successful. However, the fact that immunoprecipitaion of conditioned medium with anti-MTP 97-kDa subunit coprecipitated a large amount of apoB (Figure 3C) is compatible with a 1:1 molar ratio. Second, the secretion of MTP into the medium may result in a transient deficiency of MTP in the cell and subsequent alteration in apoB particle assembly.

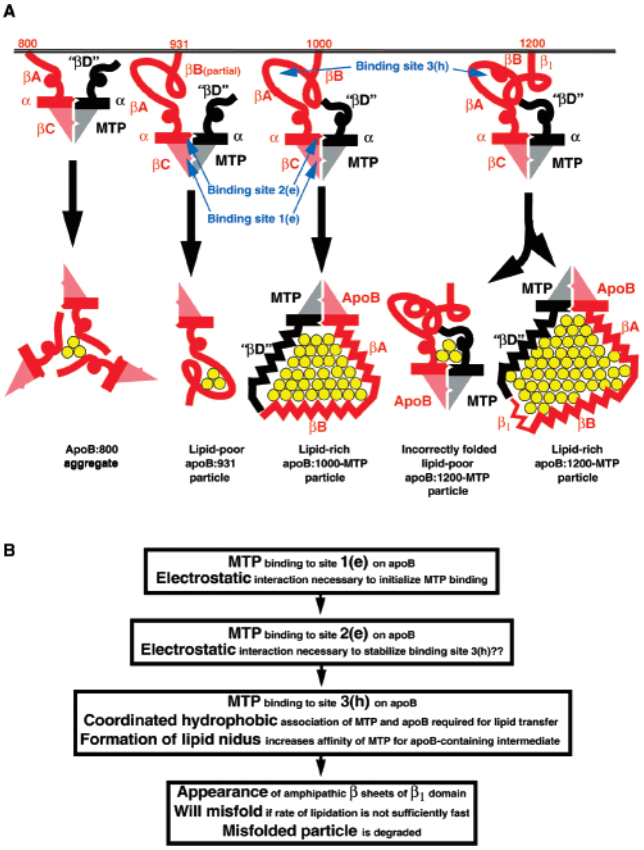


FIGURE 7: Model for the initial stages of assembly of apoB-containing particles. (A) Schematic diagram of the formation of a nascent lipid pocket intermediate. Binding site 1(e): electrostatic binding site of MTP to the $\beta$C $\beta$ barrel region of apoB near residue 200 (*10*, *22*). Binding site 2(e): electrostatic binding site of MTP to the α helical bundle region of apoB near residue 500 (*21*, *23*, *24*). Binding site 3(h): coordinated hydrophobic binding of the $\beta$B and $\beta$A amphipathic $\beta$ sheets of apoB (site 3(h)) and the amphipathic $\beta$ sheet domain of MTP (*1*) with the nascent nucleus of lipid formed by lipid transfer. (B) Four-step model for the initial stages of apoB-containing particle assembly.

One plausible explanation is that mature apoB-containing particles secreted into the medium do not contain a 1:1 molar ratio of MTP to apoB. Alternatively, it is possible that MTP secretion might serve as a regulator of apoB-containing particle assembly. We plan to investigate these possibilities in future studies.

Upon the basis of the results of this study, we propose a model for the initial stages of apoB-containing particle assembly (Figure 7A) that is substantially similar to the lipid-pocket model we previously proposed (*1*). (i) ApoB:800, due to the complete absence of the $\beta$B domain, is unable to form a lipid-pocket. MTP associates electrostatically with apoB:800 in the ER via binding sites 1(e) and 2(e) (Figure 7A, left) but dissociates from apoB:800 during significant manipulation such as ultracentrifugation.

(ii) ApoB:931, because of an incomplete $\beta$B domain, forms a lipid-pocket that associates poorly with the amphipathic $\beta$ sheet domain of MTP, preventing lipid transfer. MTP associates electrostatically with apoB:931 in the ER via binding sites 1(e) and 2(e) (Figure 7A, middle left) but dissociates from apoB:931 during significant physical manipulation to form a lipid-poor particle containing little, if any, MTP.

(iii) ApoB:1000, containing a complete $\beta$B domain, associates properly with the amphipathic $\beta$ sheet domain of MTP (*1*), allowing lipid transfer into an intact nascent lipid-pocket. We hypothesize that the bulk of lipid transfer occurs after release of the particle from the ER membrane. This is a working hypothesis that is based upon the reasonable assumption that apoB:1000 is released from the ER membrane simultaneously with completion of the lipid pocket, leaving insufficient time for completion of lipid transfer that is only initiated upon creation of the pocket. Since the particle is a trapped stable intermediate, lipidation then proceeds in the particles free within the lumen of the ER. MTP associates electrostatically with apoB:1000 in the ER via binding sites 1(e) and 2(e) and through coordinated hydrophobic binding of the $\beta$B and $\beta$A amphipathic $\beta$ sheets of apoB (site 3(h)) and the amphipathic $\beta$ sheet domain of MTP (*1*) with the nascent nucleus of lipid formed by lipid transfer (Figure 7A, middle right). Thus, MTP remains hydrophobically associated with apoB:1000 during ultracentrifugation to form a lipid-rich particle containing MTP. Alternatively, as demonstrated by Bakillah and Hussain (*36*), the MTP-lipid complexes that apparently exist in the lumen of ER may bind to apoB with higher affinity allowing the apoB−MTP complexes to remain associated during ultracentrifugation. This would imply that the first 1000 amino acid residues of apoB might be sufficient to complete the "lipid pocket" without the requirment of MTP. We do not favor this latter possibility but cannot rule it out based on our present results. We speculate that MTP may not bind to the small apoB:1000 particle when subjected to density gradient ultracentrifugation and/or NDGGE because it contains insufficient lipid to activate the largely irreversible hydrophobic 3(h) binding site.

(iv) The addition of 200 residues of the $\beta_1$ domain in apoB:1200 adds amphipathic $\beta$ strands to the growing particle. This addition appears to induce instability in particle assembly so that only a fraction of the truncated protein is correctly folded for secretion in the form of a lipid-rich particle co-associated with MTP (Figure 7A, right). A likely explanation for the bimorphic apoB:1200 results is that the particle is released from the ER membrane before significant lipidation occurs in most particles. Inadequate lipidation leads to incorrect folding of the residues of the $\beta_1$ domain in most particles, trapping MTP in an inactive form that cannot transfer lipid to lipidate the particle. Relevant to this step in the model, Ginsberg and co-workers (*37*, *38*) have suggested that the initial appearance of a portion of the lipid-associating $\beta_1$ sheet domain of apoB-100 retards translocation efficiency and/or increases susceptibility to proteasomal degradation through association with the cytoplasmic face of the ER membrane.

Studies by Carraway et al. (*39*) have demonstrated that apoB-29, apoB-32.5, and apoB-37 are secreted with peak densities of 1.25, 1.22, and 1.16 g/mL, respectively. Our apoB:1000 construct (apoB-22) secretes as its major product a 112 Å particle with a peak density of 1.208 g/mL, while apoB:1200 (apoB-26.5) secretes as its major product a 99 Å particle with a peak density of 1.24 g/mL. One way to reconcile the Carraway et al. (*39*) study with the present one is to assume that the addition of nascent amphipathic $\beta$ sheets of the $\beta_1$ domain between apoB-22 and apoB-32.5 results in the release of particle from the ER membrane before significant lipidation occurs in most particles.

Figure 7B is a flow diagram of a four-step model for the initial stages of apoB-containing particle assembly. The first step is an electrostatic interaction of MTP with site 1(e) of apoB (*10*, *22*) that is necessary for initiating MTP binding. The second step is an electrostatic interaction of MTP with site 2(e) of apoB (*21*, *23*, *24*). We have suggested elsewhere (*1*) that the binding of MTP to site 2(e) is necessary for stabilization of step 3. This step involves the coordinated hydrophobic binding of MTP and site 3(h) on apoB with a nascent nucleus of lipid formed by lipid transfer into a lipid pocket intermediate. Step 3 is supported by the present study. In step 4, biosynthesis of the amphipathic $\beta$ sheets of much of the $\beta_1$ results in the release of particle from the ER membrane before significant lipidation occurs in most particles leading to formation of misfolded particles and their subsequent degradation. This step, originally suggested by Ginsberg and co-workers (*37*, *38*), is also compatible with the present study.

## REFERENCES


1. Segrest, J. P., Jones, M. K., and Dashti, N. (1999) *J. Lipid Res. 40*, 1401−1416.
2. Raag, R., Appelt, K., Xuong, N. H., and Banaszak, L. (1988) *J. Mol. Biol. 200*, 553−569.
3. Banaszak, L., Sharrock, W., and Timmins, P. (1991) *Annu. Rev. Biophys. Biophys. Chem. 20*, 221−246.
4. Sharrock, W. J., Rosenwasser, T. A., Gould, J., Knott, J., Hussey, D., Gordon, J. I., and Banaszak, L. (1992) *J. Mol. Biol. 226*, 903−907.
5. Anderson, T. A., Levitt, D. G., and Banaszak, L. J. (1998) *Structure 6*, 895−909.
6. Segrest, J. P., Jones, M. K., Mishra, V. K., Anantharamaiah, G. M., and Garber, D. W. (1994) *Arterioscler. Thromb. 14*, 1674−1685.
7. Segrest, J. P., Jones, M. K., Mishra, V. K., Pierotti, V., Young, S. H., Boren, J., Innerarity, T. L., and Dashti, N. (1998) *J. Lipid Res. 39*, 85−102.
8. Steyrer, E., Barber, D. L., and Schneider, W. J. (1990) *J. Biol. Chem. 265*, 19575−19581.
9. Perez, L. E., Fenton, M. J., and Callard, I. P. (1991) *Comp. Biochem. Physiol. [B] 100*, 821−826.
10. Mann, C. J., Anderson, T. A., Read, J., Chester, S. A., Harrison, G. B., Kochl, S., Ritchie, P. J., Bradbury, P., Hussain, F. S., Amey, J., Vanloo, B., Rosseneu, M., Infante, R., Hancock, J. M., Levitt, D. G., Banaszak, L. J., Scott, J., and Shoulders, C. C. (1999) *J. Mol. Biol. 285*, 391−408.
11. Wetterau, J. R., Aggerbeck, L. P., Bouma, M. E., Eisenberg, C., Munck, A., Hermier, M., Schmitz, J., Gay, G., Rader, D. J., and Gregg, R. E. (1992) *Science 258*, 999−1001.
12. Wetterau, J. R., Combs, K. A., McLean, L. R., Spinner, S. N., and Aggerbeck, L. P. (1991) *Biochemistry 30*, 9728−9735.
13. Ricci, B., Sharp, D., Orourke, E., Kienzle, B., Blinderman, L., Gordon, D., Smithmonroy, C., Robinson, G., Gregg, R. E., Rader, D. J., and Wetterau, J. R. (1995) *J. Biol. Chem. 270*, 14281−14285.
14. Gordon, D. A., Jamil, H., Sharp, D., Mullaney, D., Yao, Z., Gregg, R. E., and Wetterau, J. (1994) *Proc. Natl. Acad. Sci. U.S.A. 91*, 7628−7632.
15. Jamil, H., Gordon, D. A., Eustice, D. C., Brooks, C. M., Dickson, J. K., Jr., Chen, Y., Ricci, B., Chu, C. H., Harrity, T. W., Ciosek, C. P., Jr., Biller, S. A., Gregg, R. E., and Wetterau, J. R. (1996) *Proc. Natl. Acad. Sci. U.S.A. 93*, 11991−11995.
16. Gretch, D. G., Sturley, S. L., Wang, L., Lipton, B. A., Dunning, A., Grunwald, K. A., Wetterau, J. R., Yao, Z., Talmud, P., and Attie, A. D. (1996) *J. Biol. Chem. 271*, 8682−8691.
17. Jamil, H., Chu, C. H., Dickson, J. K., Jr., Chen, Y., Yan, M., Biller, S. A., Gregg, R. E., Wetterau, J. R., and Gordon, D. A. (1998) *J. Lipid. Res. 39*, 1448−1454.
18. Patel, S. B., and Grundy, S. M. (1996) *J. Biol. Chem. 271*, 18686−18694.
19. Wu, X., Zhou, M., Huang, L. S., Wetterau, J., and Ginsberg, H. N. (1996) *J. Biol. Chem. 271*, 10277−10281.
20. Bakillah, A., Jamil, H., and Hussain, M. M. (1998) *Biochemistry 37*, 3727−3734.
21. Hussain, M. M., Bakillah, A., Nayak, N., and Shelness, G. S. (1998) *J. Biol. Chem. 273*, 25612−25615.
22. Liang, J., and Ginsberg, H. N. (2001) *J. Biol. Chem. 276*, 28606−28612.
23. Bradbury, P., Mann, C. J., Kochl, S., Anderson, T. A., Chester, S. A., Hancock, J. M., Ritchie, P. J., Amey, J., Harrison, G. B., Levitt, D. G., Banaszak, L. J., Scott, J., and Shoulders, C. C. (1999) *J. Biol. Chem. 274*, 3159−3164.
24. Hussain, M. M., Obunike, J. C., Shaheen, A., Hussain, M. J., Shelness, G. S., and Goldberg, I. J. (2000) *J. Biol. Chem. 275*, 29324−29330.
25. Segrest, J. P., Jones, M. K., De Loof, H., and Dashti, N. (2001) *J. Lipid Res. 42*, 1346−1367.
26. Yao, Z. M., Blackhart, B. D., Linton, M. F., Taylor, S. M., Young, S. G., and McCarthy, B. J. (1991) *J. Biol. Chem. 266*, 3300−3308.
27. Miller, A. D., Miller, D. G., Garcia, J. V., and Lynch, C. M. (1993) *Methods Enzymol. 217*, 581−599.
28. Dashti, N. (1992) *J. Biol. Chem. 267*, 7160−7169.
29. Laemmli, U. K. (1970) *Nature 227*, 680−685.
30. Chung, B. H., Segrest, J. P., Ray, M. J., Brunzell, J. D., Hokanson, J. E., Krauss, R. M., Beaudrie, K., and Cone, J. T. (1986) *Methods Enzymol. 128*, 181−209.
31. Burnette, W. N. (1981) *Anal. Biochem. 112*, 195−203.
32. Schumaker, V. N., Phillips, M. L., and Chatterton, J. E. (1994) *Adv. Protein. Chem. 45*, 205−248.
33. Herscovitz, H., Derksen, A., Walsh, M. T., McKnight, C. J., Gantz, D. L., Hadzopoulou-Cladaras, M., Zannis, V., Curry, C., and Small, D. M. (2001) *J. Lipid Res. 42*, 51−59.
34. Swift, L. L., Valyi-Nagy, K., Rowland, C., and Harris, C. (2001) *J. Lipid Res. 42*, 218−224.
35. Hussain, M. M., Bakillah, A., and Jamil, H. (1997) *Biochemistry 36*, 13030−13067.
36. Bakillah, A., and Hussain, M. M. (2001) *J. Biol. Chem. 276*, 31466−31473.
37. Pan, M., Liang, J., Fisher, E. A., and Ginsberg, H. N. (2000) *J. Biol. Chem. 275*, 27399−27405.
38. Liang, J., Wu, X., Jiang, H., Zhou, M., Yang, H., Angkeow, P., Huang, L. S., Sturley, S. L., and Ginsberg, H. (1998) *J. Biol. Chem. 273*, 35216−35221.
39. Carraway, M., Herscovitz, H., Zannis, V., and Small, D. M. (2000) *Biochemistry 39*, 9737−9745.
40. Sayle, R. A., and Milner-White, E. J. (1995) *Trends Biochem. Sci. 20*, 374.


BI011757L